PERGAMON

Carbon 40 (2002) 177–182

CARBON

Combustion synthesis of fullerenes and fullerenic nanostructures

Anish Goel[a], Peter Hebgen[a], John B. Vander Sande[b], Jack B. Howard[a,*]

[a]*Department of Chemical Engineering, Massachusetts Institute of Technology, 77 Massachusetts Avenue Cambridge, Massachusetts, MA 02139, USA*

[b]*Department of Materials Science and Engineering, Massachusetts Institute of Technology, 77 Massachusetts Avenue Cambridge, Massachusetts, MA 02139, USA*

Received 15 March 2001; accepted 15 June 2001

Abstract

Samples of condensable material collected from low-pressure premixed and diffusion benzene/oxygen/argon flames were analyzed chemically to determine fullerene yield and by high-resolution transmission electron microscopy to characterize the fullerenic material on and within the soot particles. Results show that fullerene formation is sensitive to changes in operating conditions, such as fuel/oxygen ratio, chamber pressure, and inert gas dilution, and that the formation of amorphous and fullerenic carbon occurs early in the flame, with the structures becoming more curved with greater residence time. All flames exhibit a fullerene maximum with the premixed flame showing two distinct regions of formation. Additionally, the fullerene maximum in the diffusion flames is always just above the stoichiometric flame surface and a maximum is observed with increasing dilution due to competing dilution effects. Image analysis data show that the curvatures and diameters of the structures are consistent with the chemical analysis and that nanostructures, found at greater residence times than fullerenes, are formed directly from curved structures in the soot. These data complement previous fullerene studies and shed light on several proposed mechanisms for fullerene formation in combustion.

Keywords: A. Fullerene; Soot; B. Combustion; C. Chromatography; Transmission electron microscopy

1. Introduction

Fullerenes were discovered by Kroto et al. in 1985 as products of carbon evaporation into an inert gas [1]. They consist of closed spherical shells comprised only of carbon atoms. This special structure results in unusual physical and chemical properties with a large potential for applications such as superconductors, sensors, catalyst, optical and electronic devices, polymers, and biological and medical applications. Fullerenes can also be formed in low-pressure fuel-rich flames of certain hydrocarbons [2–4], the highest yields being obtained under conditions of substantial soot formation. Other interesting classes of fullerenic or curved-layer carbon that can also be found in fullerene producing systems are nanostructures having tubular, spheroidal, or other shapes and consisting of onion-like or nested closed shells [5–8] and soot particles having considerable curved-layer content [9–11]. More information on the formation of fullerenic carbon in flames under different conditions is needed to understand the formation mechanisms and kinetics and to enable the design of practical systems for large-scale production.

2. Premixed flame studies

Much of the research on fullerene formation in flames has been done with low-pressure, laminar premixed flames of benzene and oxygen with or without inert diluent gas. The setup for these flames is described elsewhere [12]. In these flames, the largest yields of fullerenes were observed not under the most heavily sooting conditions, but under conditions where 2–3% of the carbon is converted to soot. With lower fuel/oxygen ratios the amount of fullerenes formed decreases to small amounts near the critical conditions for soot formation. With variations of pressure in the burning chamber, fuel/oxygen ratio, and inert gas dilution, it was possible to produce soots with wide variations in the amount of fullerenes present [3].

Subsequent studies [4] have shown that premixed flames

*Corresponding author. Tel.: +1-617-253-4574; fax: +1-617-258-5042.

E-mail address: jbhoward@mit.edu (J.B. Howard).

0008-6223/02/$ – see front matter
PII: S0008-6223(01)00170-1

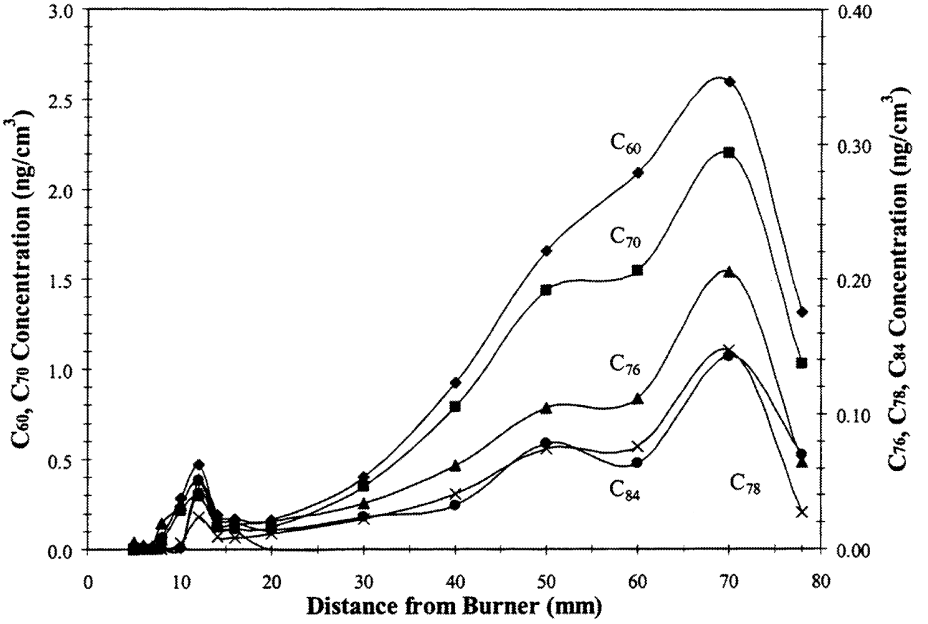

Fig. 1. Axial flame gas fullerene concentrations in a premixed benzene/oxygen/argon flame [4].

have two distinct fullerene forming regions as can be seen in Fig. 1. The second or later formation region accounts for most of the fullerenes mass produced [4]. Analyses of residence-time resolved soot samples suggest that the formation of amorphous and fullerenic carbon occurs early in the flame, with the fullerenic carbon becoming more curved as a soot particle traverses the length of the flame. Curvature of carbon layers seen in high resolution transmission electron microscopy (HRTEM) images was quantified by measuring the arc length L and diameter D of many layers and computing a curvature parameter defined as $C = L/\pi D$ which ranges from 0 for a planar layer to 1 for a completely closed spherical layer (Fig. 2). The formation of fullerenic nanostructures under premixed combustion conditions appears to require much longer residence times than the ~70 ms available in the flames [9].

3. Diffusion flame studies

Fullerenes formation in diffusion flames had received little study until recently although this type of flame, if effective, would offer advantages for practical operation. In recent work [11], fullerenes formation in laminar jet diffusion flames of benzene diluted with argon and burning in oxygen at pressures of 12 to 40 Torr was characterized. The experimental setup used to study these flames is described elsewhere [11].

The diffusion flames were characterized by measuring the ratios of the mass of fullerenes to the mass of condensable material and to the volume of non condensable gas. The results show that fullerenes, fullerenic nanostructures and fullerenic soot can form in diffusion flames with yields and extent of curvature in the soot as large as those seen in premixed flames. The results of the fullerene analysis (Fig. 3) show that every flame exhibited a fullerene maximum.

The maximum concentration of fullerenes along the axis of the flame was found just above the stoichiometric surface, near the location of the highest flame temperature and in the region where the concentration of fullerene precursors, which in flames are polycyclic aromatic hydrocarbons (PAH) [13–15], is decreasing and fullerenes are beginning to be consumed, both due to oxidation. These consumptions are presumably offset by the increase of fullerene formation rate with increasing temperature and the formation of five-membered rings in the structure of PAH through oxidation of, followed by CO elimination from, six-membered rings [16]. Surprisingly, the maximum fullerene percentage in the condensables occurs at fuel dilutions as high as 65%. The extent of soot formation decreases with increasing dilution, thereby reducing the radiative heat loss from the flame and increasing temperature until this effect is balanced by the lower production of heat due to less fuel.

The total amount of soot seems to be an important factor for the consumption of fullerenes because, at 40 Torr, the percentage of fullerenes in the condensable material is highest at the highest dilution, but the temperature is lower compared to lower dilutions. At the same time, the concentration of precursors for soot and fullerenes is

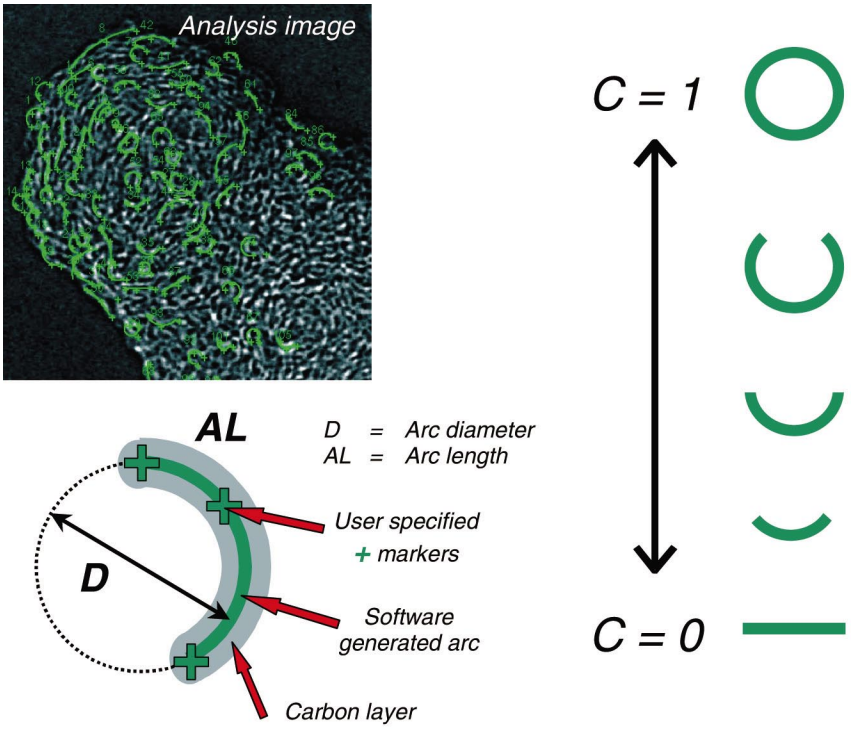

Fig. 2. Example HRTEM image with curvature parameter calculation technique.

decreasing. This makes the flame with the lowest total concentration exhibit the highest fullerene percentage. The same effect is seen with decreasing pressure. A lower pressure gives lower soot and fullerene concentrations, but the percentage of fullerenes is still higher. This behavior results in shorter flames yielding a higher percentage of fullerenes in the condensable material.

4. Discussion

The electron microscope images of soot from fullerene forming flames show a composition that is different from samples collected in higher-pressure flames or conventional combustion systems [9]. However, structures similar to those seen here have also been found in commercially-produced carbon black [17,18]. A representative HRTEM image of condensable material from a fullerene forming diffusion flame (Fig. 4) shows that both fullerenes and curved carbon layers are present. Curvature analysis of this image produces the histograms shown in Fig. 5. Comparison of such histograms obtained for samples from various distances from the burner indicates that fullerene structures, i.e., curved layers, in the soot, as characterized by the curvature parameter, increase up to the location of the fullerene maximum in the gas phase and decline thereafter. This behavior would be expected since the fullerene concentrations seen in the chemical analysis discussed above show a similar trend. The locations of the curvature peak (from HRTEM) and the fullerene peak (from HPLC) coincide.

An increase in the diameter of layers can indicate either or both of two effects, that layers are actually growing in size and/or that the layers are becoming flatter. Coupling the diameter observations with those from curvature and arc length indicates that the layers are becoming increasingly curved until the fullerene maximum in the gas phase is reached, and then start to become flat, perhaps being incorporated into nanostructures. The diameter data reinforces the conclusions drawn from the curvature data.

The amount of nanotubes and onion-like structures is higher in the diffusion flames than in the premixed flames studied. In the latter case, nanostructures were seen only at long residence times where the oxygen had been depleted. In the diffusion flames, nanostructures appear relatively soon after the stoichiometric flame surface where the maximum temperature occurs and the fullerenes and soot are being oxidized and fullerenes are being incorporated into the soot. At longer residence times, the closed structures in the soot disappear, while at the same time, we find nested structures and, separated from the soot, nanostructures. Consequently, the time-scale for nanostructure formation in diffusion flames must be shorter than that for premixed combustion. The HRTEM analysis of the soot material indicates that the nanostructures are formed directly from curved structures in the soot. An HRTEM

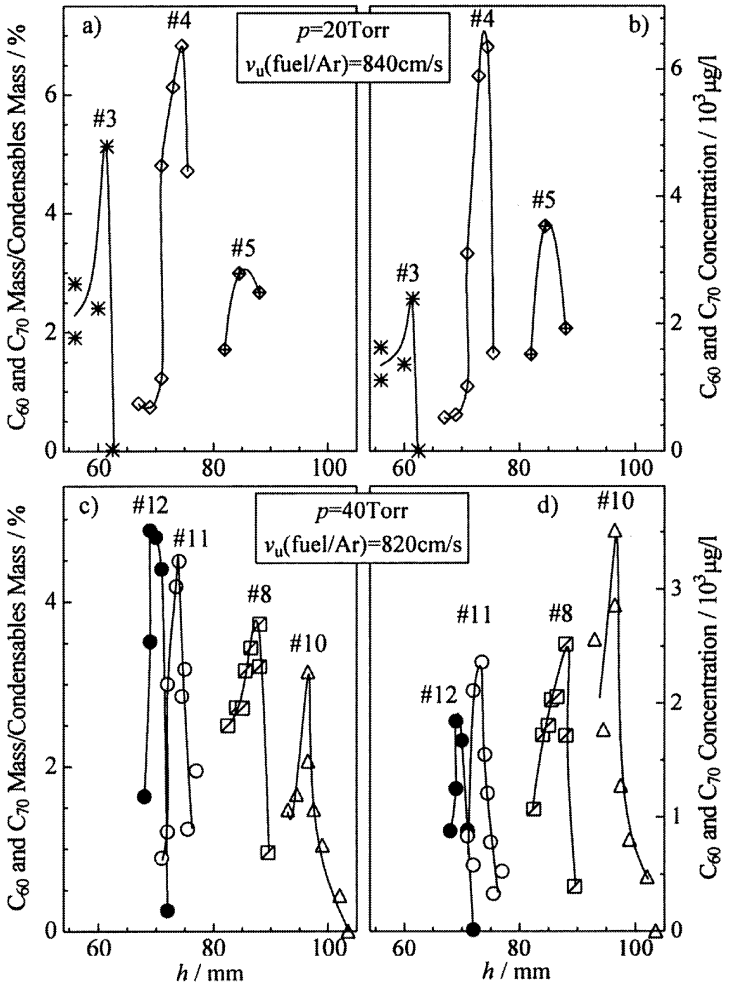

Fig. 3. Quantity of fullerenes C_{60} and C_{70} in the condensable material (a, c) and concentration of fullerenes C_{60} and C_{70} in the cold probed gas (b, d) from different heights above the burner in different flames [11].

image of fullerenic nanostructures from collected diffusion flame material is shown elsewhere [11]. In addition to fullerenic nanostructures, larger fullerene molecules have also been observed here, as in prior combustion studies [4,19,20].

Studies suggest that fullerenes are formed by reactions generating PAH which can form fullerenes as well as soot particles. Mechanisms involving carbon clusters as chains and rings have been identified in carbon vaporization production methods [21–24]. However, these mechanisms are not suitable for combustion synthesis because the concentration of these clusters is too small [20]. Consequently, several other mechanisms for fullerene formation in flames have been proposed.

Pope et al. [25] modeled fullerenes formation as stepwise acetylene addition to curved PAH, reactive coagulation of curved PAH, and hydrogen elimination followed by ring closure. Pope et al. also indicate that intramolecular rearrangements may play a role in fullerene formation.

As mentioned previously, the precursors of fullerenes and other fullerenic material may be PAH with curvature arising from embedded five-membered rings. Baum et al. [20] suggest that this is a plausible mechanism for fullerene formation as opposed to a direct route from polyynes to fullerenes. Baum et al. argue that the large rate of positive fullerene ion formation is a strong argument that PAH and their ions are precursors of fullerenes and fullerenic ions, respectively.

Also, as discussed above, gas-phase as well as condensed-phase reactions may be involved. For gas-phase synthesis, Baum et al. [20] present a zippering mechanism. In this mechanism, two large PAH molecules align so as to zip their edges together through hydrogen elimination. This mechanism also involves the simultaneous internal

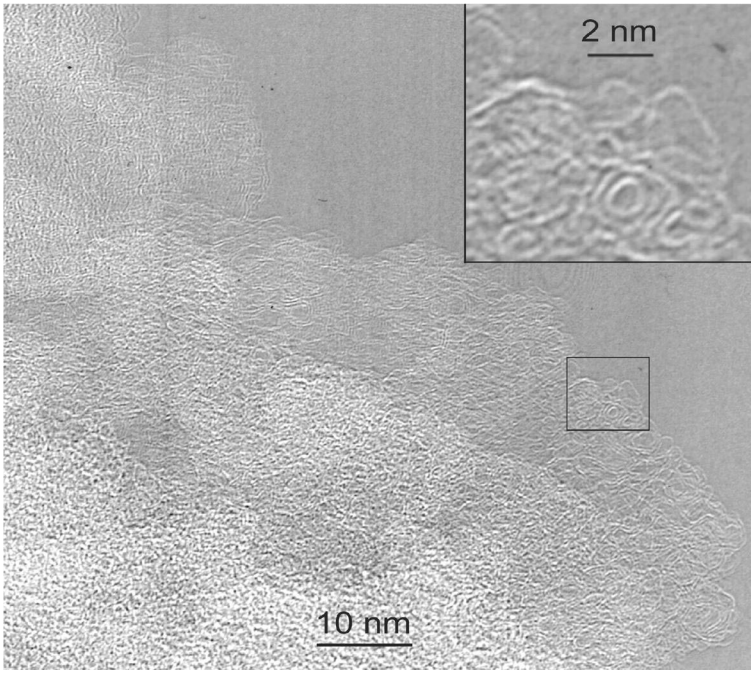

Fig. 4. HRTEM image of condensable material (pressure = 40 Torr, argon dilution = 85.3%, height above burner = 75 mm) [11].

rearrangement of the PAH to form the five-membered rings that are characteristic of fullerenes. Alternatively, the five-membered rings may already be present as it is possible that two PAH with bowl-like structures participate in the zippering mechanism [25]. Baum et al. [20] also suggest a condensed-phase mechanism in which young soot particles

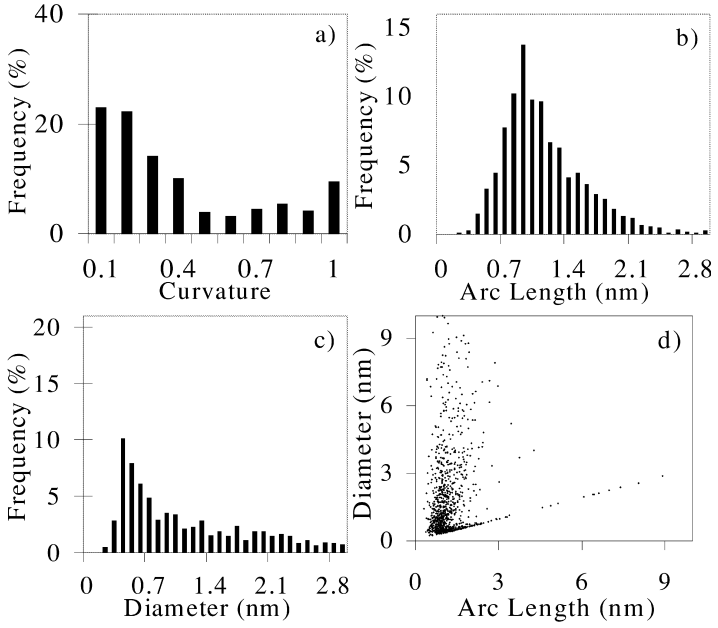

Fig. 5. Normalized histograms of curvature (a), arc length (b), diameter (c) and arc length versus diameter scatterplot (d) of condensable material (pressure = 40 Torr, argon dilution = 85.3%, height above burner = 75 mm) [11].

act as reactors for fullerenes. Surface growth of these particles and arched subunits within, along with internal rearrangement of the soot, can lead to closed shells that can then evaporate from the rest of the particle.

There are also mechanistic implications in the data presented above. It is thought that oxidation reactions are responsible both for fullerene and precursor consumption but that the highest concentrations of fullerenes occur where the precursor concentration is already decreasing [11]. This suggests that fullerene formation is also dependent on temperature as this location coincided with the highest observed flame temperature. Additionally, the presence of a fullerene maximum with respect to dilution indicates that fullerene formation is defined by the competing effects of reduced radiative heat loss and reduced heat production. Observations of longer residence times in the flames also suggest that nanostructures are formed much later than fullerenes and that fullerenes may be incorporated into the soot.

Finally, it has also been shown that pressure, temperature, fuel type, and residence time all affect the relative amounts of curved and planar PAH formed, the yield of fullerene molecules, and the relative amounts of fullerenic and graphitic carbon in the particles. In addition to experiments on pressure and temperature effects in benzene flames [4,9,11], studies have been done using fuels such as naphthalene [26], butadiene [26], toluene [27] and organics with halogen additives [28]. Of pure fuels, it was found that benzene produces the greatest amounts of fullerenes [3,11,26,27], but production could be enhanced with a chlorine additive [28]. It also appears that lower pressures and higher temperatures result in higher fullerene concentrations [11] but operating conditions have not been optimized.

Acknowledgements

We are grateful to David Kronholm for development of image analysis software, to Murray Height for preparation of Fig. 2, to Lenore Rainey for HRTEM work and to William Grieco for premixed flame data. Different parts of the work described here were supported by the National Aeronautics and Space Administration (Grant No. NAG3-1879) and the Division of Materials Sciences (Grant No. DE-FG02-85ER 45179) and the Division of Chemical Sciences (Grant No. DE-FG02-84ER 13282), Office of Basic Energy Sciences, Office of Energy Research, U.S. Department of Energy.

References

[1] Kroto HW, Heath JR, O'Brien SC, Curl RF, Smalley RE. Nature 1985;318:162.
[2] Howard JB, McKinnon JT, Makarovsky Y, Lafleur AL, Johnson ME. Nature 1991;352:139.
[3] Howard JB, Lafleur AL, Makarovsky Y, Mitra S, Pope CJ, Yadav TK. Carbon 1992;30:1183.
[4] Grieco WJ, Lafleur AL, Swallow KC, Richter H, Taghizadeh K, Howard JB. Proc Combust Inst 1998;27:1669.
[5] Iijima S. Nature 1991;354:56.
[6] Ugarte D. Carbon 1995;33:989.
[7] Howard JB, Chowdhury KD, Vander Sande JB. Nature 1994;370:603.
[8] Chowdhury KD, Howard JB, Vander Sande JB. J Mater Res 1996;11:341.
[9] Grieco WJ, Howard JB, Rainey LC, Vander Sande JB. Carbon 2000;38:597.
[10] Werner H, Herein D, Blöcker J, Henschke B, Tegtmeyer U, Schedelniedrig T, Keil M, Bradshaw AM, Schlogl R. Chem Phys Lett 1992;194:62.
[11] Hebgen P, Goel A, Howard JB, Rainey LC, Vander Sande JB. Proc. Combust. Inst. 2000;28 [in press]
[12] McKinnon JT. Ph.D. thesis, Massachusetts Institute of Technology, 1989.
[13] Ahrens J, Bachmann M, Baum T, Griesheimer J, Kovacs R, Weilmünster P, Homann KH. Int J Mass Spectrom Ion Processes 1994;138:133.
[14] Pope CJ, Marr JA, Howard JB. J Phys Chem 1993;97:11001.
[15] Lafleur AL, Howard JB, Marr JA, Yadav T. J Phys Chem 1993;97:13539.
[16] Bittner JD, Howard JB. Proc Combust Inst 1981;18:1105.
[17] Donnet JB. Rubber Chem Technol 1998;71:323.
[18] Donnet JB, Wang TK, Wang CC, Monthioux M, Johnson MP, Norman DT, Wansborough RW, Bertrand P. In: KGK Kautschuk Gummi Kunststoffe Hüthig, Heidelberg: GmbH, 1999, p. 340.
[19] Richter R, LaBrocca AJ, Grieco WJ, Taghizadeh K, Lafleur AL, Howard JB. J Phys Chem 1997;101:1556.
[20] Baum T, Löffler S, Löffler P, Weilmünster P, Homann KH. Ber Bunsenges Phys Chem 1992;96:841.
[21] Krestinin AV, Moravsky AP. Chem Phys Lett 1998;268:479.
[22] Helden GV, Hsu MT, Gotts N, Bowers MT. J Phys Chem 1993;97:8182.
[23] Hunter JM, Fye JL, Roskamp MF, Jarrold MF. J Phys Chem 1994;98:1810.
[24] Strout DL, Scuseria GE. J Phys Chem 1996;100:6492.
[25] Pope CJ, Marr JA, Howard JB. J Phys Chem 1993;97:11001.
[26] Ahrens J, Bachmann M, Baum T, Greisheimer J, Kovacs R, Weilmünster P, Homann KH. Int J Mass Spec Ion Proc 1994;138:133.
[27] Richter H, Fonseca A, Thiry PA, Gilles JM, Nagy JB, Lucas AA. In: MRS, Fall Meeting, 1994.
[28] Richter H, de Hoffman E, Doome R, Fonseca A, Gilles JM, Nagy JB, Thiry PA, Vandooren J, Van Tiggelen PJ. Carbon 1996;34:797.